CEDTECH International Journal of Engineering & Applied Science
Volume 5, Number 1, March 2024
http://www.cedtechjournals.org
ISSN: 2756-4533

FREQUENCY-DEPENDENT POLARIZABILITY AND HYPERPOLARIZABILITY OF NOVEL GERMANIUM-PHENYL NANOCLUSTER: A DFT INVESTIGATION

Njapba S. Augustine[1] and Galadanci M. S. Garba[2]
[1]Department of Physics, Gombe State University, PMB 127, Gombe State, Nigeria
[2]Department of Physics, Bayero University, Kano PMB 3011, Kano State, Nigeria

ABSTRACT

DFT calculations of molecular structure parameters of [$Ge_9(C_6H_5)$] nanostructure in the gas phase were performed using the hybrid functional B3LYP with Lanl2dz basis sets. Also, TD-DFT calculations were performed to obtain the optical properties of the nanostructure. Different parameters of the optimized structure such as the electronic properties, thermodynamic defects (i.e. vacancies and self-interstitial), dipole moment, mean polarizability, First-order hyperpolarizability and frequency-dependent first order hyperpolarizability of the energetically stable [$Ge_9(C_6H_5)$] nanostructure were calculated. The HOMO and LUMO energies are -6.229 eV and -3.563 eV respectively, with an energy band gap of 2.66 eV. The dipole moment of the nanostructure calculated was high about 7.7708 Debye. Nonlinear optical properties of the nanostructure were calculated at two levels of theory, B3LYP and CAM-B3LYP employing different frequencies. Theoretically calculated values of the static mean polarizability, anisotropic polarizability and First-order static hyperpolarizability were found to be 51.276×10^{-24} esu, 27.059×10^{-24} esu and 9.774×10^{-30} esu respectively at B3LYP which are greater than the calculated values for CAM-B3LYP level. A similar trend is observed for the Frequency-dependent parameters, polarizability and First-order hyperpolarizability. The calculated First-order hyperpolarizability of the nanocluster material is greater than the value of the standard compound Urea ($\beta = 0.343273\times10^{-30}$ esu). This result suggests germanium-phenyl [$Ge_9(C_6H_5)$] nanostructure is good as an optoelectronic device material.

Keywords: *TD-DFT, Energy band gap, Polarizability, Hyperpolarizability, Defect, Nanocluster, Nonlinear*.

INTRODUCTION.

Germanium is an important semiconductor element having use in both microelectronic industries and academics because of its excellent intrinsic electronic mobility ($\mu_e = 3900 cm^2 v^{-1} s^{-1}$), highest hole mobility (

$\mu_h = 1900 cm^2 v^{-1} s^{-1}$), suitable band gap (0.67 eV) and high absorption coefficients at the wavelengths of interest 1.3 and 1.55μm (Miya *et al*, 1979). Nowadays, germanium is still a comparatively rare element, however, one with great technological importance. Germanium clusters (small and medium size) have been investigated previously using theoretical calculations and experiments as well as structures and properties of metal-doped germanium clusters (Kikuchi *et al*, 2006; Sionani *et al*. 2019). The studies show that metal-doped Ge clusters induces novel properties such as magnetic, superconducting behaviors, photoelectric effects, thermodynamic properties and reduced energy gap between the highest occupied molecular orbital and lowest unoccupied molecular orbital(Ranjan *et al*, 2016). For theoretical calculations, techniques used typically include DFT. While pure semiconductor clusters are chemically active due to unsaturated dangling bonds, doping or combining with a foreign atom may lead to a significant enhancement of stability (Singh *et al*. 2005).

Benzene is the archetypical aromatic regular hexagon of carbon; it is planar, cyclic, fully conjugated system that possesses delocalized π-electrons. The Benzene ring is the building block for small organic molecules and polymers (Grundmann, 2016). It has the simplest structure in the aromatic hydrocarbon family. Being the smallest aromatic compound, it is a prototype of metal catalyzed production of many larger molecules with important industrial applications and has frequently been employed as a model molecular system for studies involving larger hydrocarbons aimed at characterizing the adsorption and interaction on metal surfaces (Rockey *et al*. 2006; Morin *et al*. 2004). Phenyl(Benzene molecule without one hydrogen atom) ring based molecules have been intensively studied as an electronic material because of their good conductivity due to presence of conjugated π-orbital and easy manipulation of their properties through substitution with functional groups such as amid or nitride (Woo *et al*. 2008). Many theoretical works have shown that substitution or doping of the phenyl ring by any functional group induces a substantial change to the electronic structure of the material. Priyakumar *et al*.(2002) have reported computational studies of isomers of benzene and group IV elements using *ab initio* hybrid density functional B3LYP level of theory. Considerable theoretical studies of transition metal-benzene complex $M[C_6H_6]_n$ (M = Sc-Ni) have been investigated by carrying out structure optimization of neutral, cationic, and anionic species(Pandey *et al*. 2001; Liu *et al*. 2013). Using

DFT method of calculation the results show that the metal-benzene distances, dissociation energies, ionization potential, electron affinity and spin across the 3d series of the complexes differ qualitatively. However, all of these results agree with the available experimental data.

Recently, considerable activity in the organo-germanium field investigating the interaction of the monoatom and the organic functional group emerged. The most investigated Organo-germanium compounds are the germsesquioxanes of general formula $[(GeCHR^1C3HR^2COOH)_2O_3]_n (R^1, R^2 = H, alkyl, aryl, hetaryl)$. For example the sesquioxide of 2-carboxylethylgermanium $Ge(CH_2CH_2COOH)_2O_3$ have been reported while a number of pentavalent and hexavalent germanium compounds have been synthesized and characterized by X-ray diffraction and ^{73}Ge NMR spectroscopy (Takeuchi *et al*.2004; Rosenbery, 2009). Many experimental studies on nine-atom germanium Ge_9, cluster doped with phenyl ring atoms have been reported. For example, Goicoechea and Sevov,(2006) have reported the synthesis, X-ray diffraction crystal structure characterization and spectroscopic studies of nickel-centered cluster of nine-atom germanium cluster and ligated nickel atom $Ni_2Ge_9[PPh_3]^-$.Their results revealed a nine-atom germanium Ge_9 cluster core one Ni encapsulated in the centre of the cluster and Ni (PPh_3) fragments capping the cluster. The spectrum also revealed the parent ion as well as all fragments present in the gas phase. Sun *et al*.(2009) have also reported the synthesis, experimental and theoretical characterization of $[Ni@(Ge_9PdPPh_3)]^{2-}$.

Herein, we have intensively studied the properties of novel hybrid nine-atom germanium-phenyl $[Ge_9(C_6H_5)]$ nanostructure. The nonlinear optical properties and the thermodynamic defect of this novel hybrid have been calculated. Studying and improving these properties in Germanium-Phenyl nanocluster in the gas phase is the focus of this research. Therefore, we report the results of the investigation of the properties of germanium-phenyl $[Ge_9(C_6H_5)]$ nanostructure in the gas phase using the hybrid DFT/B3LYP functional in conjunction with Lanl2dz basis set. The nine-atom germanium-phenyl $[Ge_9(C_6H_5)]$ nanostructure is a hybrid organic-inorganic material that we hope will possess interesting optoelectronic

features. Little is known about *ab initio* DFT structure parameter calculations of neutral nine-atom germanium-phenyl nanocluster.

Computational Methodology

Figure 1.1 represent the molecular structure of [$Ge_9(C_6H_5)$] nanostructure. DFT using the hybrid B3LYP functional and *ab initio* molecular orbital theory calculations were carried out to investigate the structural and electronic properties of [$Ge_9(C_6H_5)$] nanostructure. The PES scan was performed to predict the most stable molecular structure of the nanostructure using B3LYP/CEP-31g basis set. The most stable molecular structure was optimized at DFT/ MP2 and DFT/B3LYP methods with Lanl2dz basis set using Gaussian 09 program (Frisch *et al*, 2009) in the framework of unrestricted formalism. Harmonic vibrational frequencies at the optimized structure were done to confirm the optimized structure to be an energy minimum. The long-range corrected functional CAM-B3LYP was utilized to calculate within the framework of the time-dependent density functional theory, the linear and nonlinear optical properties. GaussSum 3.0(O'Boyle *et al*, 2008) was used to obtain the density of state (DOS) curves and HOMO-LUMO energy gap. The total static dipole moment(μ_i), mean polarizability $<\alpha>(-\omega, \omega)$ the anisotropic polarizability $\Delta\alpha$, and the total first hyperpolarizability β_{total} using the x, y, z components are quantities most commonly determined experimentally (Spackman, 1989). These quantities are defined as follows:

Dipole moment, $$\mu_i = \left[\mu_x^2 + \mu_y^2 + \mu_z^2\right]^{\frac{1}{2}} \quad (1)$$

Mean Polarizability, $$\langle\alpha\rangle = \frac{1}{3}\left(\alpha_{xx} + \alpha_{yy} + \alpha_{zz}\right) \quad (2)$$

Anisotropic Polarizability, $$\Delta\alpha = \frac{1}{\sqrt{2}}\left[\left(\alpha_{xx} - \alpha_{yy}\right)^2 + \left(\alpha_{xx} - \alpha_{zz}\right)^2 + \left(\alpha_{yy} - \alpha_{zz}\right)^2\right]^{\frac{1}{2}} \quad (3)$$

First-order Hyperpolarizability, $$\beta = \left[\beta_x^2 + \beta_y^2 + \beta_z^2\right]^{\frac{1}{2}} \quad (4)$$

where $\beta_x = \beta_{xxx} + \beta_{xyy} + \beta_{xzz}$, $\beta_y = \beta_{yyy} + \beta_{xxy} + \beta_{yzz}$, $\beta_z = \beta_{zzz} + \beta_{xxz} + \beta_{yyz}$.

DFT is a reasonably accurate and efficient technique for the predictions of energies and structures. It has been applied in the calculations of polarizability and hyperpolarizability (Ye and Autschbach, 2006; Rice *et al*, 1990). These parameters are computed for static and dynamic cases using first principles based approach with DFT/CAM-B3LYP functional and Lanl2dz basis sets and results are compared with experiment where

necessary. The Gaussian 09W software will be used to calculate the dipole moment (μ_i), polarizability and first order hyperpolarizability using the finite field approach.

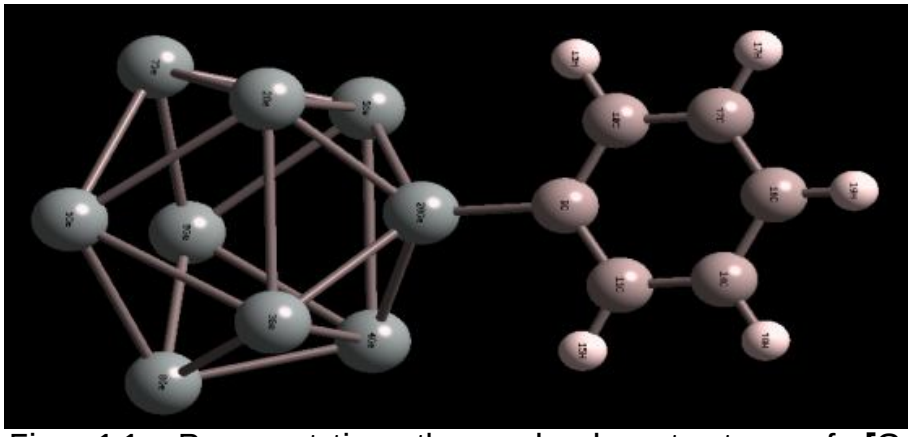

Figure1.1**:** Representation the molecular structure of **[**$Ge_9(C_6H_5)$] nanostructure
(Njapba and Galadanci, 2021).

RESULTS AND DISCUSSIONS

Frontier Orbital Analysis, IP and EA of [$Ge_9(C_6H_5)$] nanostructure

Most of a materials behavior such as intrinsic conductivity, optical transition or electronic transitions depends on the energy gap. Thus, any change of this parameter will significantly alter the materials physics and chemistry. Between the highest occupied molecular orbital (HOMO) and the lowest unoccupied molecular orbital (LUMO) is the energy gap (E_g). This parameter characterizes molecular chemical stability and it is a critical parameter in determining molecular electrical transport properties, for example the electronic conductivity. The calculated energy gap, i.e. the HOMO and LUMO energies are listed in Table 1.1. It is observed from Table 1.1 that the nine-atom germanium-phenyl [$Ge_9(C_6H_5)$] nanostructure has an energy gap of about 2.66 eV(i.e. 6.229-3.36 eV). This means the charges in the valence band need more energy to transit to the conduction band. In contrast, low values of the energy gap require less energy to move charges from valence band to conduction band. The solid state experimental energy gap value of Ge is reported as 0.67eV (Sze, 1981; Yu and Cardona, 1996; Grundmann, 2016). Our calculated value is far higher than the experimental value. However, it is still a semiconductor since it falls within the semiconductor range. The increase in the gap energy arises

from the electronic configuration of the aromatic elements as well as the theoretical methodology. In addition, the localization of charges is high in the valence band than in the conduction. This localization of charges in the nanostructure can be visualized from the density of state spectrum as reported in literature.

Table 1.1: Calculated energy, HOMO, LUMO, Dipole moment, and Point Group of $Ge_9(C_6H_5)]$.

Compound	Energy /eV	Dipole Moment/D	Point Group	HOMO /eV	LUMO /eV	IP /eV	EA /eV	E_g / eV
Pure Ge_9	-911.284	0.7399	C_1	-	-			-
Phenyl $C_6H_5)$	-6314.816	-0.0009	C_1	-	-			-
$Ge_9(C_6H_5)$	-7203.450	7.7708	C_1	-6.229	-3.563	6.229	3.563	2.67

IP is the energy required to dislodge an electron from the nanostructure and EA is the energy released due to the addition of electrons to the nanostructure. EA plays a vital role in chemical sensors and plasma physics. According to Koopman's theorem of molecular orbitals, IP and EA are defined as follows (Zhan *et al*, 2003):

$$IP = -E_{HOMO} \quad , \quad EA = -E_{LUMO} \tag{5}$$

The IP and EA are shown in Table 1.1**.** It is observed that IP of the nanostructure is about 6.229 eV, which is high. This implication is that more energy will be required to remove an electron from the cluster and consequently cannot actively participate in a chemical reaction. The EA has a value of 3.563 eV. This value suggest that moderately small amount of energy can be released due to the addition of electrons in $[Ge_9(C_6H_5)]$. Also, this value can provide information about the active participation in a chemical reaction process.

Binding energy (BE) and Chemical Stability of $[Ge_9(C_6H_5)]$ nanostructure

The Binding energy of the nine-atom germanium-phenyl $[Ge_9(C_6H_5)]$ nanostructure is calculated using the following expression(Sriram and Chandiramouli, 2013):

$$BE = \frac{nE(Ge_9) + mE(C_6H_5) - E(Ge_9C_6H_5)}{n+m} \tag{6}$$

where $E(Ge)$ is the energy of Ge atoms, $E(C_6H_5)$ is the energy of the phenyl atoms, n and m are number of atoms of germanium and the phenyl atoms respectively. The binding energy provides information about the binding of the atoms in the cluster. It also gives the precise data about the stability of the nanostructure. As depicted from Table 1.1, the calculated binding energy is found to about -413.5 meV. Significantly, this value shows the nanostructure is stable having a tricapped trigonal planar structure. Also, the calculated energy for pure germanium, phenyl and nine-atom germanium-phenyl [$Ge_9(C_6H_5)$] nanostructure are -911.284, -6314.816, and -7203.453 eV respectively. The stability of the nanostructure gradually increases with an increase in the number of atoms. This variation in the calculated energy arises due to change in the electronic configuration of the nine-atom germanium and the phenyl atoms. The dipole moment is observed to be 0.0009, 0.7399 and 7.7708 Debye respectively for phenyl, nine-atom germanium and [$Ge_9(C_6H_5)$] nanostructure. The low values for the phenyl and the nine-atom germanium indicates that the atoms are well packed and the charges present inside the clusters are uniformly distributed. In contrast, for nine-atom germanium-phenyl [$Ge_9(C_6H_5)$] nanostructure, its dipole moment is about 7.7708 Debye. There is an uneven charge distribution i.e. in one direction more than the other. This value may significantly contribute towards its activity. The point group of all the simulated clusters is C_1. This point group refers to asymmetry in the structure.

Thermodynamic Defects

The formation energy of defects $H^f_{I,V}$, vacancies (V) and self-interstitials (I) of the nine-atom germanium-phenyl [$Ge_9(C_6H_5)$] nanocluster were obtained from the Gaussian 09 output file of a frequency calculation based on first principle approach. We have considered defects in the nine-atom germanium and in germanium-phenyl nanostructure. The formation energies of vacancies and self-interstitials obtained from DFT calculations are shown in Table 1.2 As can be seen from Table 1.2, the enthalpy vacancy formation energy was calculated to be 1.75 eV, far lower than the formation energy of self-interstitial, 3.70 eV. Claeys and Simoen,(2007) reported calculated values of formation energies for vacancy and self-interstitials as 1.93 eV and 2,29 eV respectively in Ge using DFT calculations.

Table 1.2: Enthalpy vacancy formation H_V^f and self-interstitial H_I^f (in eV) of $[Ge_9(C_6H_5)]$ at B3LYP/Lanl2dz basis sets.

Material	Defect-type	H^f (eV)
Ge_9	V	1.75
	I	3.70
$Ge_9(C_6H_5)$	V	1.85
	I	3.78

These values are in good agreement with other studies that predict vacancies formation energies to be in the range of 1.7-2.2 eV and self-interstitial formation energies in the range of 2.3-4.1 eV (Spiewak *et al*, 2007). Furthermore, it can be seen that H_V^f are always lower than H_I^f. Pinto *et al*, (2006) has reported that the dominant intrinsic defect in a material is the vacancy due to its lower formation energy. This lower energy suggests it can play an important role in germanium as primary mediating specie for self-diffusion and diffusion of impurities (Werner *et al*, 1985; Bracht *et al*, 1991). Ge has high mobility of electrons and holes when compared to other group IV elements and with low formation energy it would not be surprising to find vacancy clusters forming easily in the material. Indeed, large voids have been reported with diameters ranging from hundreds of nanometers up to ten micrometer following the growth of Ge crystals and such voids could severely damage devices if they form within the active region (Poelman *et al*, 2004; Hens *et al*, 2005). Similarly, for the germanium-phenyl nanostructure the formation enthalpy of self-interstitials H_I^f is greater than the formation enthalpy of vacancy H_V^f calculated at 298 K and one atmosphere. Ramanarayanan and Cho, (2003) reported theoretical calculated value of formation energy of vacancy for germanium compound as 1.88 eV.

Considering the effect of temperature to electronic devices, we have varied the temperature in the range $300-900\ \mathrm{K}$ for our defect nanostructure material for vacancy and self-interstitial.

Table 1.3: Formation Enthalpies of Vacancies (V) and Self-interstitial (I) at different Temperatures.

T / K	H_V^f (eV)	H_I^f (eV)
300	1.21	2.38
400	1.41	3.79
500	1.62	3.94
600	1.64	4.43
700	1.65	4.79
800	1.67	4.92
900	1.70	5.10

As followed from the data of Table 1.3 and Figure 1.2, the formation enthalpy of self-interstitials of the nanostructure is higher than the vacancies. Both vacancies and self-interstitials increase with increasing temperature. The vacancies increase uniformly with respect to temperature, while self-interstitials changes rapidly with temperature. However, vacancies are missing atoms and are the simplest defect in semiconductor materials. Higher temperature increase vibrational motion and expand the crystal, hence more vacancies are formed at higher temperatures. Pinto *et al*, (2006) suggested that high temperature vacancy in Ge hybrids differ in properties from low temperature hybrids. Interstitials are atoms displaced from their normal location that appear in one of the interstitics in the lattice. Here the distortion spread at least a few layers in the crystal. In most cases, the number of defects is much smaller than the number of vacancies. These defects in crystalline solids can thus effectively act as trapping centre of charge carriers and have significant effect on electrical conductivity of devices. With regard to Ge clusters, self-interstitial defects are less important as compared to vacancy due to its significantly higher formation enthalpy energy H_I^f (Spiewak *et al*, 2008). Several experimental studies have confirmed greater number of vacancies present in Ge at varied temperatures due to dopant behavior (Claeys and Simoen, 2007; Brotzmann *et al*, 2008). In germanium quite all dopant diffuse through a mechanism mediated by vacancies (Bracht and Brotzmann, 2006; Huger *et al,* 2008). Spiewak *et al*, (2008) report that self-diffusion is dominant in germanium complexes and play important role in dopant diffusion. Impurities are also very necessary in semiconductor

materials and are typically assisted by vacancies or self-interstitials. From our knowledge of semiconductors, the elements of group III and V are the most common impurities used by group IV semiconductors particularly Si and Ge (Wada and Kimerling, 2015).

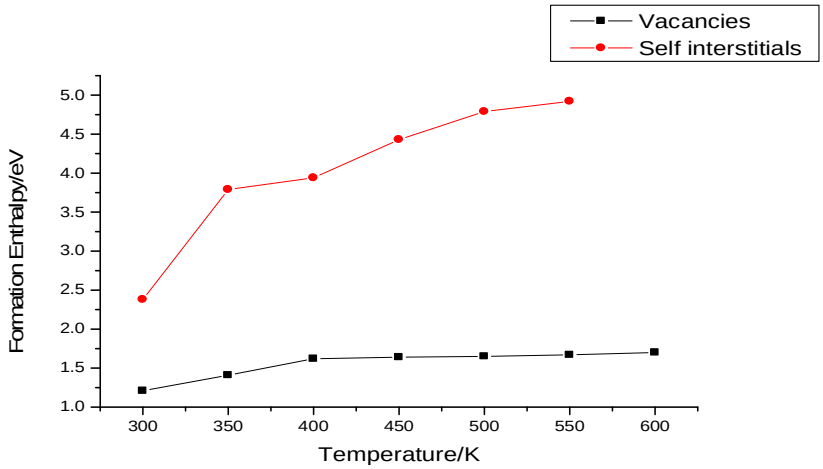

Figure 1.2: Temperature dependence of the Formation Enthalpy of vacancy and self-interstitial $H_{I,V}^{f}$ of $[Ge_9(C_6H_5)]$.

These impurities interact with defects in germanium complex single crystal. Boron (B), Gallium (Ga), Phosphorus (P), Arsenic (As) and Antimony (Sb) are important dopant for germanium-based technologies. In this light, we investigated the interaction of these impurities with nine-atom germanium-phenyl $[Ge_9(C_6H_5)]$ nanostructure by calculating their binding energy. The binding energy is calculated using the equation above and the results are shown in Table 1.4.

Table 1.4: Calculated Binding energies of impurities in $[Ge_9(C_6H_5)]$.

	B	P	As	Sb
$E_b(eV)$	-0.7	-0.7	-0.8	-0.8

The negative values of the binding energy implies that the vacancies are stable for B, P, As, and Sb with respect to the constituent point defect components. The more negative the value, the stronger the interaction between the dopant atom and the nanostructure. If $E_b \geq 0$, the interaction

is repulsive and the dopant atom may detached from the nanostructure after overcoming all the bond-breaking barriers. Furthermore, the stability is almost remaining constant despite the increase in atomic radius of the dopant. The behaviors are twofold; nine-atom germanium is quite heavy as well as the phenyl group. Consequently, the influence of the dopant elements is insignificant.

Static and Frequency-dependent Polarizability and Hyperpolarizability

Table 1.5 depicts the results of static and dynamic molecular electric properties i.e. the dipole moment (μ), polarizability (α), first hyperpolarizability (β) as well as frequency-dependent polarizability $\alpha(-\omega;\omega)$ and first order hyperpolarizability $\beta(-\omega;\omega,0)$ for the nine-atom germanium-phenyl [$Ge_9(C_6H_5)$] nanocluster where both values are measured in electrostatic units(10^{-30} esu). We employed DFT in our calculations with the CAM-B3LYP functional and the results were compared with typical B3LYP functional values. We used the Lanl2dz basis set in our calculations. For the purpose of studying the response behavior, we carried out the frequency-dependent polarizability and first hyperpolarizability at optical frequencies of $\omega = 0.02389$, 0.04282 and 0.0774 atomic units (a.u). Most employed the finite field approach, however, fewer studies have used the coupled-perturbation Hartree-Fock (CPHF) scheme which we have used in the present study as implemented in Gaussian 09 program package. The dipole moment, polarizability, anisotropic polarizability ($\Delta\alpha$) and first hyperpolarizability have been calculated. Table 1.2 shows the calculated dipole moment (μ), mean polarizability $\langle\alpha\rangle$, anisotropic polarizability ($\Delta\alpha$), first hyperpolarizability (β) and the frequency-dependent polarizability and first hyperpolarizability.

It can be found from Table 1.2 that the calculated total dipole moment is equal to 7.7452Debye. The highest value is observed for the x-component, i.e. $\mu_x = 7.7451$D other component values being $\mu_y = 0.0260$D and $\mu_z = 0.0344$D respectively. So, there is more charge distribution in the x-direction than other directions. The higher the dipole moment the stronger is the inter-molecular interaction. This value for [$Ge_9(C_6H_5)$] may significantly contribute towards its activity. The dipole moment of the nine-atom germanium-phenyl nanostructure is approximately six times greater than that Urea(μ of Urea is only 1.3732 D, obtained by B3LYP/6-

31G(d,p) method(Muthu *et al*, 2014). Urea is one of the prototypical molecules used in the study of non-linear optical properties of molecular materials. Therefore it is used commonly as a threshold value for comparative purpose. The polarizability (α) have non-zero values and is dominated by the diagonal components. The total mean values of polarizability and anisotropic polarizability were calculated to be 50.4325×10^{-24} esu and 22.9932×10^{-24} esu respectively at CAM-B3LYP. Also, total mean polarizability and anisotropic polarizability calculated at B3LYP are respectively 1.65% and 15.03% higher in comparism to the values calculated at CAM-B3LYP. The First order hyperpolarizability of the nine-atom germanium-phenyl nanocluster calculated at CAM-B3LYP and B3LYP level of theory are almost identical i.e. 9.756×10^{-30} and 9.774×10^{-30} esu respectively. These values are dominated by longitudinal components, β_{zzz}. This implied that a substantial delocalization of charges is in that direction. The Frequency-dependent polarizability ($\alpha(-\omega;\omega)$) and first order hyperpolarizability $\beta(-\omega;\omega,0)$ are calculated at $\omega = 0.02389$, 0.04282 and 0.0774 a.u respectively to illustrate frequency- dependence. Calculations show that the total mean polarizability $\alpha(-\omega;\omega)$ increases from 50.388×10^{-24} esu to 53.29272×10^{-24} esu for germanium-phenyl nanocluster at CAM-B3LYP level and similarly for B3LYP level. However, the total anisotropic frequency-dependent polarizability $\Delta\alpha(-\omega;\omega)$ increases from 22.9932×10^{-24} esu to 26.06838×10^{-24} esu, drop and then increases again as illustrated in Figure 1.3.

Frequency-dependent first hyperpolarizability $\beta(-\omega;\omega,0)$ was calculated at both levels of theory and showed similar behavior. For CAM-B3LYP method, the values increase from 5.286×10^{-30} to 34.069×10^{-30} esu then decreases to 3.104×10^{-30} esu. The trend observed for B3LYP though with higher values of the first order hyperpolarizability $\beta(-\omega;\omega,0)$ increases from 20.2766×10^{-30} esu to 31.1248×10^{-30} esu, drop to 24.6396×10^{-30} esu and increases rapidly to 110.7558×10^{-30} esu respectively. Figure 1.3 shows the first order hyperpolarizability plotted as function of frequency. The observed large values of $\beta(-\omega;\omega,0)$ is a measure of the nonlinear optical activity associated with intramolecular charge transfer resulting from the electron cloud movement through the π-conjugated framework of the nanostructure.

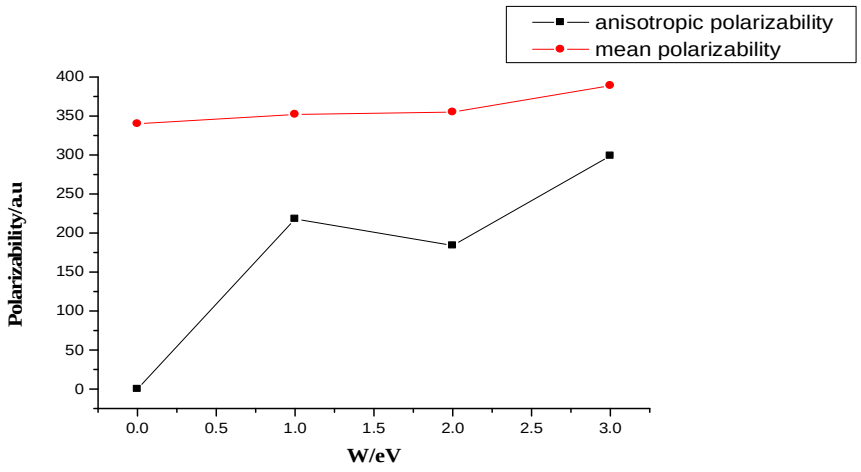

Figure 1.3: Frequency-dependent Polarizability and anisotropic Polarizability [$Ge_9(C_6H_5)$] at CAM-B3LYP Level

The First hyperpolarizability of the nine-atom germanium-phenyl nanocluster are approximately $15,99$, and 9times far greater than Urea(β for Urea is 343.273×10^{-33} esu obtained at B3LYP/6-31G(d,p) level). The values of $\beta(-\omega;\omega,0)$ for [$Ge_9(C_6H_5)$] nanocluster are larger than the corresponding static β_{total} values and exhibit larger frequency dispersion effects. The calculated results of polarizability and first order hyperpolarizability confirm that [$Ge_9(C_6H_5)$] nanocluster is a good nonlinear optical material and can be used for laser device fabrication.

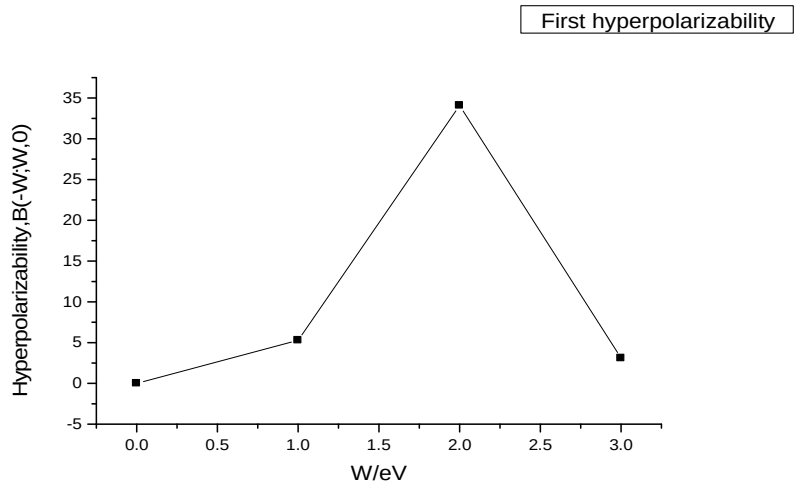

Figure 1.4: Frequency-dependent First order Hyperpolarizability $\beta(-\omega;\omega,0)$ calculated at CAM-B3LYP/Lanl2dz basis sets.

CONCLUSION

In this present study, the molecular properties of nine-atom germanium-phenyl nanocluster have been investigated at DFT/B3LYP functional with LANL2DZ basis set. The optimized geometry, vibrational frequencies, thermodynamic defect formation parameters and nonlinear optical properties of the nanocluster have been calculated. Furthermore, TD-DFT calculations were performed to obtain the optical properties of the nanostructure. The HOMO and LUMO energies predict electronic transition of electrons. The results showed that the nine-atom germanium-phenyl [$Ge_9(C_6H_5)$] nanostructure has an energy gap of about 2.66 eV(i.e. 6.229-3.36 eV). The calculated results revealed that the IP and EA values of the nine-atom germanium-phenyl [$Ge_9(C_6H_5)$] nanostructure are 6.229 eV and 3.563 eV respectively. . The nanostructure is stable. The formation energy of defects $H_{I,V}^{f}$, vacancies and self-interstitials of the nine-atom germanium-phenyl [$Ge_9(C_6H_5)$] nanocluster were calculated based on first principle approach. It is observed that the defect nine-atom germanium-phenyl [$Ge_9(C_6H_5)$] nanostructure formation energies of vacancies and self-interstitials are 1.85 eV and 3.78 eV moderately higher than that of defect nine-atom germanium formation energies of vacancies and self-interstitials of 1.75 eV and 3.70 eV respectively. For the purpose of studying the response behavior, the frequency-dependent polarizability and first hyperpolarizability at optical frequencies of $\omega = 0.02389$, 0.04282 and 0.0774 atomic units (a.u) were calculated. Frequency-dependent first-order hyperpolarizability $\beta(-\omega;\omega,0)$ was calculated at two levels, CAM-B3LYP and B3LYP with values of 5.286×10^{-30}, 34.069×10^{-30}, 3.104×10^{-30} and 20.2766×10^{-30}, 31.1248×10^{-30} 24.6396×10^{-30} esu respectively.

					Frequency(ω)			
Polarizability(α)	CAM-B3LYP	B3LYP	CAM-B3LYP	Polarizability(α)	0.0	0.02389	0.04282	0.0774
α_{xx}	442	467		α_{xx}	442	466	442	459.9
α_{yy}	306	297		α_{yy}	306	319	316	318
α_{zz}	273	274		α_{zz}	273	271	307	301
$\langle\alpha\rangle$	340.3	346		$\langle\alpha\rangle(-\omega;\omega)$	340	352	355	359.6
$\Delta\alpha$	155.15	182.59		$\Delta\alpha(-\omega;\omega)$	155	175.9	131	151
Dipole moment, μ				Hyperpolarizability β				
μ_x	7.7451	7.1036		β_{xxx}	-133.9	-133.9	3247.6	-129.3
μ_y	0.0260	0.0000		β_{yxx}	-311.7	-311.7	-767.6	-25.9
μ_z	0.0344	0.0000		β_{zxx}	776.7	776.8	-2071.1	-360.0
μ_{total}	7.7452	7.1036		β_{yyy}	42.9	42.9	-47.5	101.2
Hyperpolarizability, β				β_{zyy}	209.9	209.9	-179.2	-37.8
β_{xxx}	8.6178	-14.879		β_{zzz}	-453.5	-453.5	166.9	71.1
β_{xxy}	-0.9796	0.0000		$\beta_{total}(-\omega;\omega,0)$	611.85	611.85	3943.58	359.33
β_{xyy}	-31.8258	-36.806		$\beta_{total}(-\omega;\omega,0)\times(10^{-30}esu)$	5.286	5.286	34.069	03.104
β_{yyy}	-0.9189	0.0000	**B3LYP**	**Polarizability(α)**				
β_{xyz}	4.4367	7.311		α_{xx}	467	468	481	588
β_{yyz}	0.9910	0.0000		α_{yy}	297	288	312	306
β_{xzz}	-89.6824	-91.190		α_{zz}	274	226	285	274
β_{yzz}	0.5370	0.0000		$\langle\alpha\rangle(-\omega;\omega)$	346	327.3	359.3	389.3
β_{zzz}	-0.4478	0.0000		$\Delta\alpha(-\omega;\omega)$	182.59	217.7	183.9	299.3
β_{xxz}	0.2253	0.0000		Hyperpolarizability β				
β_{total} (a.u)	112.9	113.11		β_{xxx}	2330.1	-2324.6	2423.1	-12813
$\beta_{total}(esu)\times10^{-30}$	9.756	9.774		β_{yxx}	-0.0002	54.0	0.0002	0.00392

				β_{zxx}	-0.0006	67.8	-0.0003	0.00589
				β_{yyy}	-113.7	587.5	-399.2	-181.4
				β_{zyy}	271.2	19.6	44.6	4.498
				β_{zzz}	-528.5	-2764	-1494.9	-386.7
				$\beta_{total}(-\omega;\omega,0)$	2347.02	3602.7	2852.0	12820.2
				$\beta_{total}(-\omega;\omega,0)\times(10^{-30}esu)$	20.28	31.12	24.64	110.75

Table 1.5: Dipole moment, Polarizability and First order Hyperpolarizability data for[$Ge_9(C_6H_5)$] Nanostructure Calculated at CAM-B3LYP and B3LYP levels with Lanl2dz basis sets.

First-order hyperpolarizability of the nine-atom germanium-phenyl nanocluster are approximately $15,99$ which is 9 times far greater than Urea(β for Urea is 343.273×10^{-33} esu obtained at B3LYP/6-31G(d,p) level. The calculated results of polarizability and first order hyperpolarizability confirm that [$Ge_9(C_6H_5)$] nanocluster is a good nonlinear optical material and can be used for laser device fabrication.

REFERENCES

Bracht H. and Brotzmann S. (2006). Atomic Transport in Germanium and the Mechanism of Arsenic Diffusion. *Material Science Semiconductor Processing*, **9**, pp471–476

Bracht H., Stolwijk N. A. and Mehrer H.(1991). Diffusion and Solubility of Copper, Silver and Gold in Ge. *Physical Review B, Vol.43, no. 18 pp465-477*.

Brotzmann S., Bracht H., Lundsgaard J. H., Nylandsted A. L., Simoen E., Haller E. E., Christensen J. S. and Werner P.(2008). Diffusion and Defect Reaction between Donors, C, and Vacancies in Germanium: Experimental Results. *Physics Review B,77,pp235207 (1)-235207(13).*

Claeys C. and Simoen E.(2007). Germanium-based Technologies: From Materials to Devices, Elsevier, New York.

Frisch, M. J., Trucks, G.W., Schlegel, H. B., Scuseria, G. E., Robb, M.A., Cheeseman, J. R., Scalmani, G., Barone, V., Mennucci, B., Petersson, G.A., Nakatsuji, H., Caricato, M., Li, X., Hratchian, H. P., Izmaylov, A. F., Bloino, J., Zheng, G., Sonnenberg, J. L., Hada, M., Ehara, M., Toyota, K., Fukuda, R., Hasegawa, J., Ishida, M., Nakajima, T., Honda, Y., Kitao, O., Nakai, H., Vreven, T., Montgomery, J. A., Jr., Peralta, J. E., Ogliaro, F., Bearpark, M., Heyd, J. J., Brothers, E., Kudin, K. N., Staroverov, V. N., Kobayashi, R., Normand, J., Raghavachari, K., Rendell, A., Burant, J. C., Iyengar, S. S., Tomasi, J., Cossi, M., Rega, N., Millam, J. M., Klene, M., Knox, J. E., Cross, J. B., Bakken, V., Adamo, C., Jaramillo, J., Gomperts, R., Stratmann, R. E., Yazyev, O., Austin, A. J., Cammi, R., Pomelli, C., Ochterski, J. W., Martin, R. L., Morokuma, K., Zakrzewski, V. G., Voth, G. A., Salvador, P., Dannenberg, J. J., Dapprich, S., Daniels, A. D., Farkas, Ö., Foresman, JB., Ortiz, JV., Cioslowski, J. Fox, DJ. **2009. Gaussian 09, Revision E.01, Gaussian, Inc., Wallingford CT.**

Goicoechea J.M. and Sevov C. S.(2006). Chemistry of Deltahedral Zintl Ions. *Organometallic*, 25:5678-5692.

Grundmann M.(2016). The Physics of Semiconductors: An Introduction including Nanophysics and Applications, 3th Edition Springer, Berlin.

Helgaker J., Jaszunski M., Ruud K.(1999). Ab Initio Methods for the Calculation of NMR Shielding and Indirect Spin-Spin Coupling Constants. *Chemical Review, Vol. 99, no.1, pp293-352.*

Hens S., Vanhellemont D., Poelman D., Clauws P., Romandic I., Theuwis A., Holsteyns F., Steenbergen J. V.(2005*). Applied Physics Letters, 87, 061915*

Huger E., Tietze U., Lott D., Bracht H., Bougeard D., Haller E. E., and Schmidt H.(2008) Self-Diffusion in Germanium Isotope Multilayer at low Temperatures. *Applied Physics Letters*, **93** (16), 162104

Kikuchi H., Masae T., Yoshiyuki K (2006). Theoretical Investigation of Stable Structures of Ge_6 Clusters with Various Negative Charges: *Computational Material Science and Engineering IV. Vol.47, No.11*

Liu W., Carrasco J., Santra B., Michaelides A., Scheffler M., Tkatchenko A.(2013). *New Journal of Physics, Vol.15 pp053046*

Miya T., Teraunuma Y., Hosaka T., Miyashite T.(1979). Ultimate Low loss Single Mode Fibre at 1.55 μm. *Electron. Lett, 15 pp106-108*

Morin C., Simon D., Santet P.(2004). *Journal Physical Chemistry Vol.108, pp12084.*

Muthu S., Rajamani T., Karabacak M., Asiri A. M.(2014). Vibrational and UV Spectra, First Order Hyperpolarizability, NBO, and HOMO-LUMO analysis of 4-Chloro-N- (2- Methyl-2-3-dihydroindol-1-yl)-3-Sulfamoyl Benzamide. Spectrochimica-Acta Part A. *Molecular and Biomolecular Spectroscopy, 122, pp1-14*

Njapba A. S. and Galadanci G.S.M. (2021). Electronic Structure, Optical and Thermodynamic Properties of Germanium-Phenyl Nanocluster in the Gas-phase: A DFT Study. *International Journal of Engineering and Applied Science*.Vol.2, Number 1, pp1-31.

O'Boyle N. M., Tenderholt A. L. and Langner K. M."Cclib (2008): A Library for Package- Independent Computational Chemistry Algorithms," *Journal of Computational Chemistry*, Vol. 29, no. 5, pp839–845 . .

Pandey R., Bijan K.R., Purusottam J., Miquel A.B.(2001). Electronic Structure and Properties of Transition-Metal Benzene Complexes. *Journal American Chemical Society, Vol.123 no.16, pp3799-3808*

Pinto H., Coutinho J., Torres V., Oberg S., Briddon P.(2006). Formation Energy and Migration barrier of a Ge Vacancy from ab initio Studies. *Material Science Semiconductor Process 9(4), pp498-502.*

Poelman D., De Gryse O., De Roo N., Janssens O., Clauws P.(2004). Characterization of Bulk Microdefects in Ge Single Crystals. *Journal Applied Physics,Vol.96,no. 11 pp6164- 6168*

Priyakumari U. D., Dinadaya T.C., Narahari S.(2002). A Computational Study of the Valence Isomers of Benzene and their Group IV Hetero-analogs: *New Journal of Chemistry, 26*.

Ranjan P., Kumar A., Chakraborty T.(2016). Computational Investigation of *Ge* Doped Au Nanoalloy Clusters. A DFT Study. *Material Science and Engineering*, 149 pp1-8.

Rice J. E., Sanz J., Roger D. A., Susan M. C. and Nicholas C. H. (1990). Frequency- Dependent Hyperpolarizability with Application to Formaldehyde and Methyl Fluoride. *Journal Chemical Physics 93, no.2 pp8825-8839*.

Rockey T.J., Yang M., Dai. H. (2006*). Physical Chemistry B. Vol.110, pp19973*

Singh K. A., Kumar V.,Kawazoe Y.(2005). Thorium encapsulated caged Clusters of Ge : $Th@Ge_n (n = 16, 18 \text{ and } 20)$. *Journal Physical Chemistry B, 109,pp15187-15189*

Siouani C., Mahtout S., Rabilloud F.(2019). Structure, Stability and Electronic Properties of Niobium-Germanium and Tantalum-Germanium Clusters. *Journal of Molecular Modeling, 25, 113, pp1-17. Springer*

Spackman M. A. (1989). Accurate Prediction of Static Dipole Polarizability with Moderately Sized Basis Sets. *Journal Physical Chemistry, 93, pp7594-7603*

Spiewak P., Muzyk M., Kurzydloski K. J., Vanhellemont J., Mlynarczk K., Wabinski P., Romandic I.(2007). Molecular Dynamics Simulation of Intrinsic Point Defects in Germanium*. Journal Crystal Growth, 303, pp12-17, Elsevier*.

Spiewak P., Vanhellemont J., Sueoka K., Kurzydłowski K. J., and Romandic I. (2008) First Principles Calculations of the Formation Energy and Deep Levels Associated with the Neutral and Charged Vacancy in Germanium. *Journal Applied Phys*ics **103** (8), 086103.

Sriram S. and Chandiramouli R. (2013).A Study on the Electronic Properties of $GaInPAs$ Nanostructure. A DFT Approach. *European Physical Journal Pius, 128, pp1161-1168*

Sun Z. M., Zhao Y. F., Li J., Wang L. S.(2009). Diversity of Functionalized Germanium Zintl Clusters: Syntheses and Theoretical Studies of

$[Ge_9PdPPh_3]^{3-}$ and $[Ni@(Ge_9PdPPh_3)]^{2-}$ *Journal of Cluster Science*, Vol. 20, pp602-609, Springer.

Sze S. M. (1981), Physics of Semiconductor Devices, 2nd Edition, John Wiley and Sons, New York.

Wada K. and Kimerling L. C.(2015). Photonics and Electronic with Germanium, Wiley-VCH, Germany.

Werner M., Mehrer H., and Hochheimer H. D.(1985) Effect of hydrostatic pressure, temperature and doping on self-diffusion in germanium. *Physics Review B*, **32**, pp3930–3937,

Woo Y.K., Young C.C., Kwang S.K.(2008). Understanding Structures and Electronic/ Spintronic Properties of Single Molecules, Nanowires, Nanotubes, and Nanoribbons towards the Design of Nanodevices. *Journal of Material Chemistry, 18,pp4510-4521*.

Ye A. and Autschbach J. (2006). Study of Static and Dynamic First Hyperpolarizability using TD-DF Quadratic Response Theory with Local Contribution and Natural bond Orbital Analysis. *The Journal of Chemical Physics 125, 234101-1-12*.

Zhan C. G., Nicholas J. A., Dixon D. A.(2003). IP, EA, Electronegativity, Hardness and Electron Excitation Energy. Molecular Properties from DFT Orbital Energies. *Journal Physical Chemistry* A, 107, pp4184-4195.

Zhao W. J., and Wang Y. X.(2008). Geometries, Stabilities and Electronic Properties of $FeGe_n(n=9-16)$ Clusters: Density Functional theory Investigation. *Chemical Physics*, Vol. 350, pp291-296